Formation of nanoripples in Al films during O_2^+ sputtering

P. Mishra and D. Ghose*
Saha Institute of Nuclear Physics, Sector-I, Block-AF, Bidhan Nagar, Kolkata 700064, India
(Received 28 December 2005; revised manuscript received 6 July 2006; published 24 October 2006)

Off-normal ion bombardment of solid targets often leads to development of periodically modulated structures on the eroded surface. For tilted incidence ($\theta \geqslant 30^\circ$) of 16.7 keV O_2^+ ion beam on Al thin films, quasiperiodic ripple topography has been found to develop on the sputtered surface. As predicted by Bradley-Harper theory, below a critical angle $\theta_c \simeq 60°$, the ripple wave vectors are found to be oriented parallel to ion beam projection, while for angles above θ_c the ripple wave vectors are perpendicular to the ion beam projection. At the critical angle of ripple rotation, one observes moundlike morphology, the growth of which is similar to that of parallel ripples. It is noted that the intrinsic roughness of the film surface plays an important role in the smoothing and roughening kinetics at the early stages of sputtering.

DOI: 10.1103/PhysRevB.74.155427 PACS number(s): 79.20.Rf, 68.35.Bs, 61.80.Jh

I. INTRODUCTION

Bombardment of solid surfaces with energetic ions, besides causing sputtering of target atoms, results in pronounced topography evolution. It has been shown both theoretically and experimentally that off-normal ion bombardment leads to the formation of periodically modulated structures (ripples) on the surface of the eroded material.[1,2] The phenomenon of ripple formation has attracted much research interest in recent years both for understanding the underlying mechanism as well as for potential applications in the field of nanotechnology since sputtering can lead to spontaneous creation of patterns on the surface of many materials which can further be exploited for various technological applications. So far the formation of sputter ripples has been reported on ion bombarded surfaces of amorphous materials,[3] semiconductors,[4,5] graphite,[6] and metals,[7,8] all considering surfaces of bulk samples. Recently, we have shown that spontaneous ripple formation can also take place on a number of ion bombarded polycrystalline thin films[9,10] which have wider impact on technological applications. Generally, the ripple structures are interpreted on the basis of Bradley and Harper (BH) theory[1] where the interface instabilities caused by sputtering erosion compete with slow surface diffusion. The most important aspect of the BH theory is that the orientation of the ripples should change with the angle of ion incidence. Makeev *et al.*[2] developed morphological phase diagrams for the parameters characterizing the sputtering process where ripples with various characteristics form. It is shown that for small angles of incidence the ripple wave vectors are aligned along the ion beam direction, while at large angles of incidence the orientation changes perpendicular to the beam direction. The boundary between the two morphological regions depends critically on the shape of the collision cascade, thus on the bombarding ion energy and ion/target masses. There are a few experimental reports[3,8,11,12] where the change in orientation of the ripples as a function of ion incidence angle occuring in the same physical system has been studied. In the present paper, we report the development of ripples on Al thin films under 16.7 keV O_2^+ ion bombardment at various angles of incidence and show the rotation of the ripple pattern as the incidence angle is changed. The characteristics of the ripples, namely, the wavelength and amplitude have been studied as a function of projectile fluence. The growth of surface morphology at the critical angle of ripple rotation is also studied.

II. THE BRADLEY-HARPER MODEL OF SPUTTER RIPPLE FORMATION

According to Sigmund[13] if an ion is incident nonnormally on a surface, since it has a finite range, the maximum sputtering effect will not occur at the very point of impact, but further "downstream." The ion deposits its energy into a region of ellipsoidal shape, which is characterized by the mean penetration depth a and the longitudinal and lateral straggling widths σ and μ, respectively. The deposited energy is very much sensitive to the local surface curvature provided that the ion depth is much less than the radius of curvature. Sigmund[13] showed that on a length scale of the order of the penetration depth of the ions, the surface elevation erodes more slowly than a depression. It is also known that the surface curvature induces gradients in the chemical potential to drive mass transport away via surface diffusion from the elevated regions of the solid towards depression.[14] Combining these two counteracting effects, Bradley and Harper[1] developed a linear equation for the time evolution of the surface profile $h(\mathbf{r},t)=h(x,y,t)$ as follows:

$$\frac{\partial h}{\partial t} = -v_0(\theta) + v_0'(\theta)\frac{\partial h}{\partial x} + \frac{fa}{n}Y_0(\theta)\left[\Gamma_x(\theta)\frac{\partial^2 h}{\partial x^2} + \Gamma_y(\theta)\frac{\partial^2 h}{\partial y^2}\right] - B\nabla^4 h. \quad (1)$$

Here the projection of the ion beam on the surface is considered to be in the x direction. $v_0(\theta)$ is the rate of erosion of the unperturbed flat surface at an angle θ between the surface normal and incident beam direction. $v_0'(\theta)$ is the velocity of the perturbed surface, f is the incident projectile flux, n is the atomic density of the target, $Y_0(\theta)$ is the sputtering yield of a surface inclined at θ. $\Gamma_{x,y}$ are effective surface tension coefficients caused by the sputter process. B is a coefficient which depends on the surface self-diffusivity, the free energy per unit area, and the number of atoms per unit area moving across the surface. Equation (1) can be solved in Fourier

space. We define h_k as the Fourier transform of the surface height and $\mathbf{k}$ as the surface wave vector of interest. The general solution for a periodic perturbation is of the form

$$h_k = -v_0(\theta)t + A\exp[i(k_x x + k_y y - \omega t) + r_k t], \quad (2)$$

where k_x, k_y, ω, and r_k are real. Substituting Eq. (2) in Eq. (1) we obtain the growth rate

$$r_k = -(fa/n)Y_0(\theta)[\Gamma_x(\theta)k_x^2 + \Gamma_y(\theta)k_y^2] - B(k_x^2 + k_y^2)^2. \quad (3)$$

In principle, waves of all wave vector values can develop but the selection of the dominant wave vector is determined for which the rate of amplitude increase is maximum. The wavelength that maximizes r_k is given by

$$\Lambda = 2\pi\sqrt{\frac{2nB}{faY_0(\theta)|\Gamma(\theta)|}}. \quad (4)$$

Here $\Gamma(\theta)$ is the larger of the two negative surface tension coefficient values $-\Gamma_x(\theta)$ and $-\Gamma_y(\theta)$. At moderate incidence angles the ripples are directed perpendicular to the ion beam plane (x-direction ripples) as $\Gamma_x < \Gamma_y < 0$, while at grazing incidence angles ($\Gamma_y < 0, \Gamma_x > 0$) the ripples are aligned parallel to the ion beam plane (y-direction ripples). There exists a sharp boundary between these two regions. The critical angle θ_c above which the the ripple wave vector rotates to 90° can be determined from the condition $\Gamma_x(\theta_c) = \Gamma_y(\theta_c)$. These coefficients can be calculated from the energy deposition parameters of depth and straggles as prescibed in the literature.[1,2]

In the BH theory the diffusion mechanism is considered to be of thermal origin, which is quite feasible for metals at room temperature. It may be noted that the diffusive term $-B\boldsymbol{\nabla}^2(\boldsymbol{\nabla}^2 h)$ may be modified by the presence of grain boundaries or the misalignment of neighboring crystallites. One should also consider the effect of step-edge barriers, which, however, seems to not be prominent in the present experiment since the wavelength of the ripples is found to be larger than the grain sizes.

III. EXPERIMENTAL

Thin films of Al of nominal thickness 200 nm were prepared on a clean Si(100) substrate by dc magnetron sputtering. X-ray diffraction measurements show that the films were polycrystalline in nature. The prominent crystallites were (111) and (200) and their average dimensions were, respectively, 45 and 37 nm. These samples were sputtered with mass analyzed 16.7 keV O_2^+ ions in a low energy ion beam (LEIB) system developed in the laboratory.[15] The angle of ion incidence with respect to the surface normal, θ, was varied in the range 0–85°. The beam current density was in the range 2.5–20 μA/cm^2 depending on the angle of incidence. The projectile fluence was varied in the range 5×10^{16} O atoms/cm^2 to 5×10^{17} O atoms/cm^2 and measured by a current integrator (Danfysik, model 554) after suppression of the secondary electron emission. The base pressure in the target chamber was less than 8×10^{-8} mbar. The surface morphology of the ion-irradiated surface was examined in a MMSPM NanoScope IV (M/S Veeco, USA) both by tapping and contact modes at ambient conditions.

For the quantitative analysis of the ripple morphology, we have calculated numerically the height-height autocorrelation function $C(\mathbf{r}) = \langle[h(\mathbf{r})h(0)]\rangle$, where $h(\mathbf{r})$ is the relative surface height at the position $\mathbf{r}$ and $\langle\ \rangle$ denotes an average over all positions and directions. If one plots the one-dimensional autocorrelation function along the wave vector, it will show well-defined satellites due to the periodicity of the rippled surface. The mean ripple wavelength Λ is defined as the separation between the central peak and the first secondary correlation maximum. We have also calculated the root-mean-square (rms) roughness or the interface width $w = \sqrt{\langle[h(\mathbf{r}) - \langle h(0)\rangle]^2\rangle}$, directly from the atomic force microscope (AFM) images. The rms roughness provides a measure for the ripple amplitude. The data represent the arithmetical average of typically three or more scans on different positions of the sample, with error bars representing the standard deviation. It may be noted that the error bars in some data points are smaller than the size of the plotting symbol and thus do not appear explicitly.

IV. RESULTS AND DISCUSSION

A. Orientation of the ripples as a function of angle of incidence

Figure 1 shows some representative AFM images of the surface sputtered at different angles of incidence. The power spectral densities (PSD) calculated from the Fourier transform of the respective images are also shown in the inset. It can be seen that the ripples start to develop prominently from $\theta > 30°$. In the angular range $30° < \theta < 60°$, the ripple wave vector is found to be parallel to the ion beam direction, whereas for $\theta > 60°$, the ripples are formed with the wave vector perpendicular to the beam direction. The orientation changes can also be verified from the PSD images where the initial circular spot around $\mathbf{k}=0$ splits into two bright spots with the wave vector parallel to the ion beam direction. As θ approaches 60°, the two spots merge together and become a single circular bright spot indicating the roughening being dominant equally in both x and y directions. Further increase of θ separates the two spots again, but the orientation is now rotated by 90° with respect to the previous one thus confirming the BH prediction. A close inspection of the successsive morphologies developed at $\theta = 55$, 60, and 63°, respectively, reveals clearly that the critical angle of transition θ_c from parallel ripples to perpendicular ripples is very close to 60°. In passing, we should mention that the orientation of the ripples is found to be completely determined by the ion beam direction and no effect of azimuthal rotation of the target is observed.

The magnitude of θ_c is dictated by the spatial distribution of deposited energy, i.e., the parameters a, σ, and μ. The SRIM simulation[16] can be used to calculate the mean penetration depth a. However, the values of straggling parameters are not easy to extract from SRIM. For small θ, expanding $\Gamma_x(\theta)$ and $\Gamma_y(\theta)$ to second order in θ, it can be shown[1] that $\Gamma_x(\theta)$ will be less than $\Gamma_y(\theta)$ when the following condition is satisfied:

$$\left(\frac{a}{\sigma}\right)^2 + \left(\frac{\sigma}{\mu}\right)^2 \geq 3. \quad (5)$$

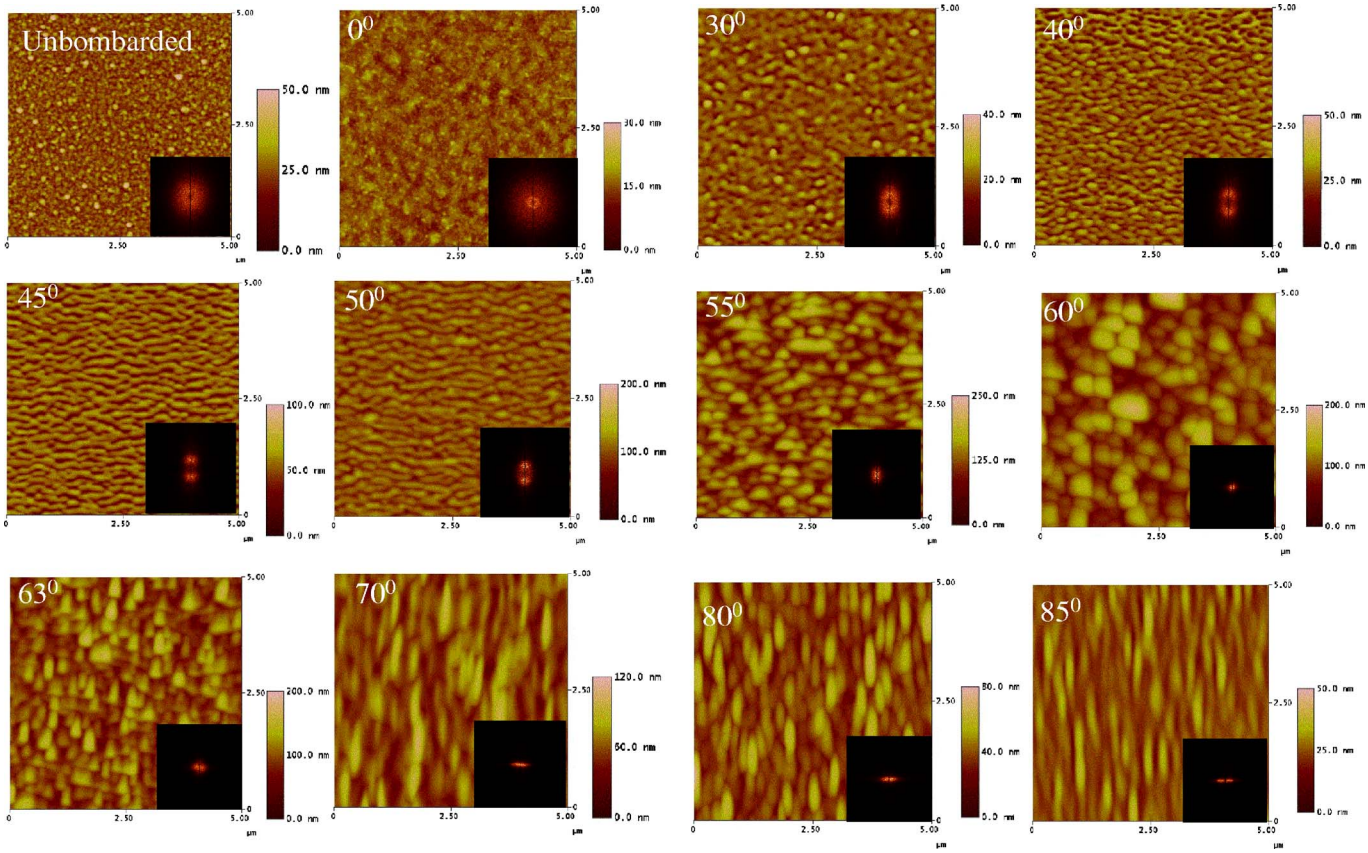

FIG. 1. (Color online) AFM images showing a sequence of the evolution of the surface topography of the Al film with increasing bombarding angle. The insets represent the corresponding 2D FFTs. The projectile is 16.7 keV O_2^+ with a fluence of 2×10^{17} O atoms/cm^2. The ion incidence angles corresponding to each micrograph are indicated. The projected ion beam direction is from the bottom to the top.

Two cases may be considered. The first one is the symmetric distribution of deposited energy, i.e., $\sigma=\mu$. The above condition is met when $a/\sigma \geqslant \sqrt{2}$. That means for smaller reduced energy depths a/σ, ripples will also appear along the y direction at low angles of incidence.[2] Such a result is somewhat unphysical and has not been reported so far. On the other hand, if one assumes an asymmetric distribution such that $\sigma \geqslant \sqrt{3}\mu$, the ripples will always be directed along the x direction for small θ even for small enough a/σ values consistent with most experimental observations. A typical damage cascade may be characterized by $\sigma=a/2$ and $\mu=a/4$ as proposed by Bradley and Harper.[1] Bolse[17] prescribed a method to calculate the deposited energy depth distribution function $F_D(x)$ by using the SRIM code. A 16.7 keV O_2^+ ion sputters the Al surface as two O atoms with half the incident ion energy, for which Bolse's recipe yields $a=11.9$ nm and $\sigma=11$ nm. In order to calculate μ, we assume that θ_c corresponds to the point of intersection of the two functions Γ_x and Γ_y. A value of $\mu=4.5$ nm fits well to the experimental value as shown in Fig. 2, which is quite a reasonable estimate when compared with the damage data of Winterbon *et al.*[18] under the present experimental conditions.

Figure 3 shows the rms surface roughness w measured over sampling areas of 5×5 μm^2 as a function of the angle of ion incidence θ. The roughness of the bombarded surface first decreases from the initial surface roughness followed by a sharp increase with θ, showing a maximum around $\theta=60°$. After that w again decreases as θ approaches the grazing angles. The sputter deposited film surface is found to be microscopically rough consisting of closely spaced conelike structures (cf., Fig. 1). Because of the angular dependence of the sputtering yield[19] the surfaces with higher local incidence angles will be eroded faster than the surroundings and a

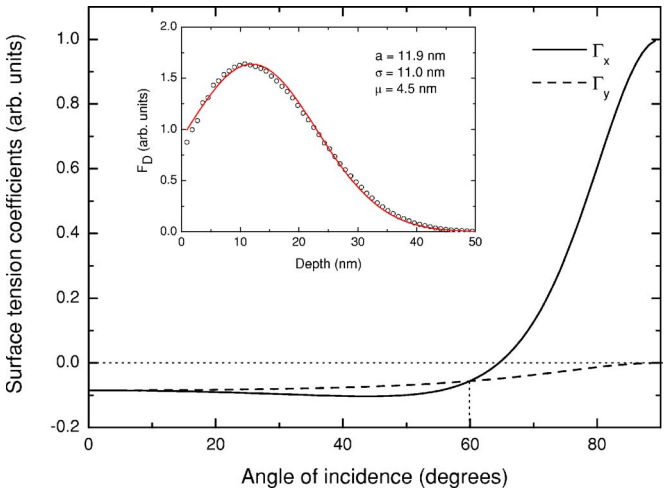

FIG. 2. (Color online) The angular dependence of the surface tension coefficients as calculated from the BH theory. The depth distribution of the deposited energy as simulated with SRIM code is shown in the inset.

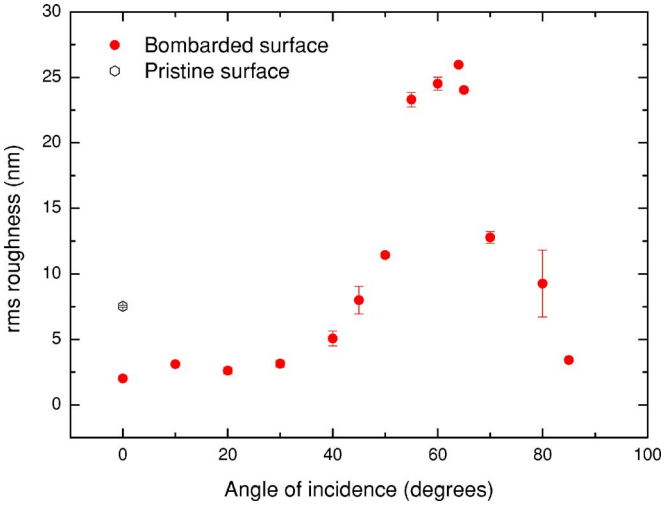

FIG. 3. (Color online) Showing the dependence of the rms surface roughness w on the ion incidence angle θ during 16.7 keV O_2^+ ion sputtering of the Al film with a fluence of 2×10^{17} O atoms/cm^2.

smoothing of the surface can be observed with time. From the section analysis of the topography we estimate the inclined angles of the sides of the cones with respect to the base being in the range 10–15°. Following a simple geometric consideration as described in Refs. 20 and 21, under the assumption that the maximum sputter etching occurs around 80°, it can be shown that such a process of ion beam smoothing is particularly effective at near grazing incidence angles ($\geqslant$70°). These conelike asperities are of a sufficiently large aspect ratio (height/lateral dimension) that the BH mechanism apparently could not operate at the very early stages of sputtering. Once the asperities are removed by erosion, the curvature-related instability begins to be relevant and ripples appear.

It is noted that at lower incidence angles ($\theta\leqslant30°$), the ripple morphology does not develop. This is not unexpected because both the negative surface tension coefficients are almost equal at near-to-normal ion incidence angles (cf., Fig. 2). Probably the angular range $0°<\theta<30°$ represents a slower regime where ripples would appear at longer sputter times. In another approach, Carter and Vishnyakov[22] have added an extra smoothing term of the form $|A(E,\theta)|\nabla^2 h$ in Eq. (1). This term is based on the anisotropic diffusion of recoil-sputter-adatoms parallel to the surface and is shown to be dominant over the erosion instability for small values of θ at a given ion energy E.

B. Evolution of parallel ripples as a function of projectile fluence

Here we have studied the evolution of ripples sputtered at θ=45°. In this region both Γ_x and Γ_y are negative, while $|\Gamma_x|$ is greater than $|\Gamma_y|$. As a result roughening grows in the x direction faster than in the y direction and ripples form with their wave vector oriented along the ion beam direction. The wavelength and amplitude of the ripples as a function of bombarding oxygen fluence ϕ are displayed in Fig. 4. Ini-

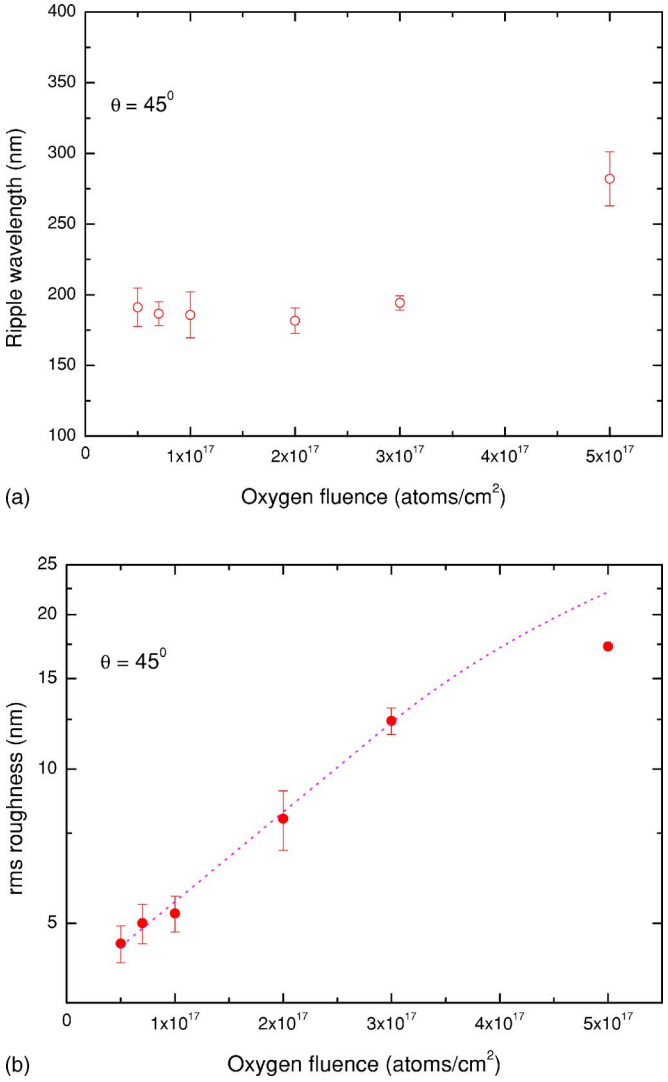

FIG. 4. (Color online) The fluence dependence of (a) ripple wavelength Λ and (b) ripple amplitude w for parallel ripples (θ =45°). The dashed line in (b) corresponds to the exponential growth.

tially the wavelength shows no significant change with fluence as demanded by the BH theory, but it tends to increase at fluences $>3\times10^{17}$ O atoms/cm^2. On the other hand, the ripple amplitude ($\propto$ rms roughness w) grows fast exponentially in the early stages followed by a slower rate of growth later indicating the effect of nonlinear processes.[23] The dashed line represents the least square fit to the experimental data in the linear regime by an exponential function $w\sim\exp\left(\frac{\phi}{\phi_0}\right)$ with $\phi_0\simeq2.5\times10^{17}$ atoms/cm^2. Dividing the incident oxygen projectile flux by ϕ_0, the growth rate of ripples is found to be about 5.7×10^{-4} s^{-1} under the present experimental conditions.

C. Evolution of perpendicular ripples as a function of projectile fluence

At grazing angles only Γ_y is negative. Since the negative surface tension coefficients are the origin of instability,

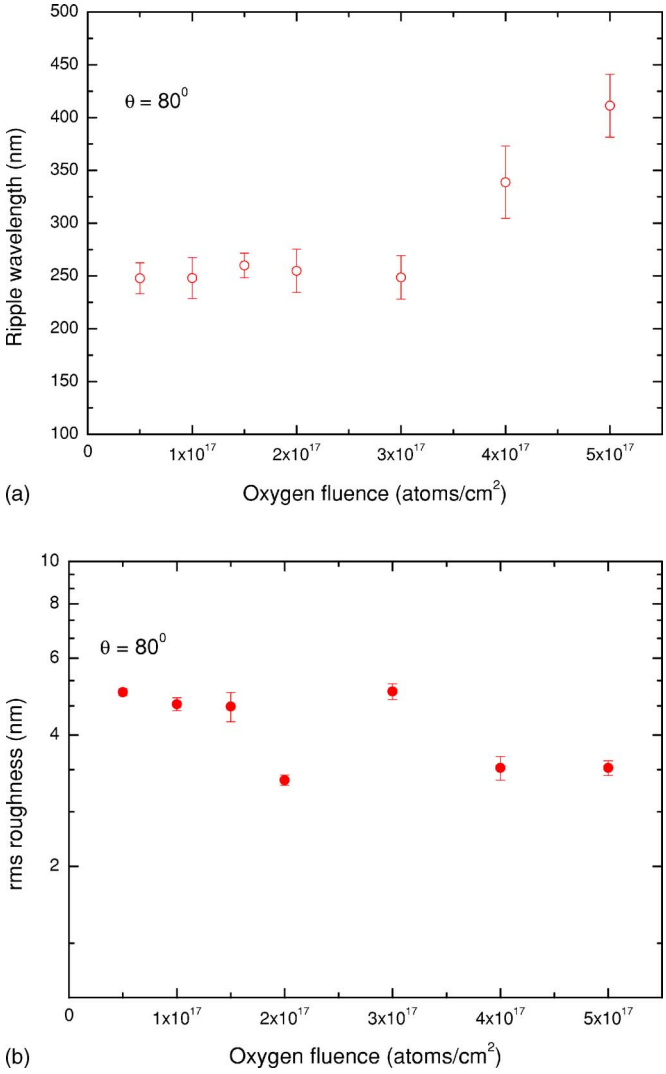

FIG. 5. (Color online) The fluence dependence of (a) ripple wavelength Λ and (b) ripple amplitude w for perpendicular ripples (θ=80°).

ripples along the y direction are developed. Figure 5 shows the plots of wavelength Λ and the rms roughness w data as a function of oxygen fluence ϕ for θ=80°. Here also the characteristic wavelength is more or less invariant at lower fluences, but it increases at higher fluences. The most interesting observaion is, however, that the roughness amplitude is largely insensitive to the fluence in the range investigated and is less than the initial surface roughness [Fig. 5(b)]. This is in contrast to the prediction of BH theory. Probably BH mechanism is involved in the early nucleation stage until other mechanisms such as redeposition and self-sputtering become important. The latter one is thought to be a potential candidate for damping of ripple morphology at higher angles of incidence.[24,25] The emitted sputtered particles, which are energetic enough, preferentially erode the peaks than the valleys thereby causing suppression of ripple growth.[25]

At angles close to grazing the increasing importance of ion reflection cannot be ignored. At this stage there is a possibility of deviation of the true collision cascade shape from a Gaussian ellipsoid.[26] The effect of ion reflection is, however, not easy to incorporate into continuum equations. Alternatively, one can study the sputter rippling by computer simulation employing Monte Carlo (MC) methods where the effects of ion reflection and shadowing of ions by surface structures are taken into account.[27,28] In these cases, the growth of ripples is found to be very much sensitive to the choice of the diffusion term and the efficiency of relaxation. Stepanova and Dew[27] have demonstrated that the vertical height fluctuations (amplitude) of the ripples may not increase with erosion time when an irreversible relaxation mechanism at relaxation rates higher than a certain threshold value is applied. This type of relaxation is generally applicable to samples at low temperatures. At room temperature or higher, thermally activated diffusion is more feasible, for which the morphology may behave differently.

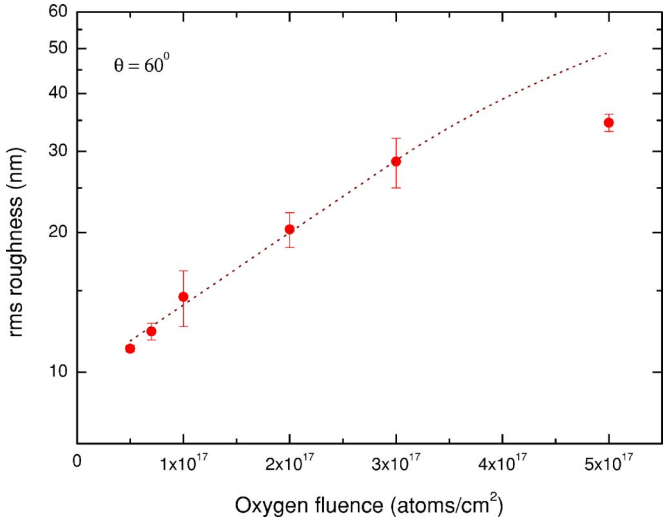

FIG. 6. (Color online) The rms amplitude w of the mound morphology developed at θ=60° as a function of oxygen fluence. The dashed line corresponds to the exponential growth.

D. Morphology evolution at the critical angle θ_c

For sputtering at $\theta=\theta_c$, Γ_x and Γ_y are equal; the erosion fails to select any preferred direction. In this case, the growth of parallel and perpendicular ripples will be overlapped. If the amplitude of each orientation is roughly equivalent, a moundlike morphology is expected to develop at the surface as found in the present experiment. Although no long range coherence is observed, the roughness should increase exponentially with a dominant correlation length. Figure 6 shows the evolution of the roughness parameter as a function of the oxygen fluence at θ_c=60°. Here also w increases exponentially with a similar growth rate as that of parallel ripples.

V. SUMMARY

In summary, the oblique angle 16.7 keV O_2^+ ion bombardment of Al thin films leads to four distinct phases in the surface-topography evolution depending on the angle of ion incidence. The ripple-topography appears at incidence angles $\theta \geqslant 30°$. In the angular range 30 to 60°, ripples are formed with wave vectors parallel to the incident ion beam projec-

tion on the surface. While for grazing ion incidence, i.e., $\theta > 60°$, ripples are formed with wave vectors perpendicular to the incident beam direction. The transition angle for the change of ripple orientation under the present sputtering conditions is found to be very close to 60°. Although the dynamics of parallel ripples largely follow the BH mechanism, the perpendicular ripples exhibit a deviation from the features of BH instability, probably some damping mechanisms, e.g., self-sputtering being dominant at large angles of incidence. At the critical angle of ripple rotation, one observes the development of moundlike morphology consistent with the behavior predicted by the instability theory of Bradley and Harper.[1] It is noted that at very early stages of sputtering the BH mechanism could not work, because of the microscopic roughness of the initial surface the local angle-dependent sputtering prevails over the curvature-dependent sputtering leading to smooth surfaces. At later times, when the surface protrusions are shaved off, the erosion driven destabilization starts to be relevant and the ripple structures form on the surface. Finally, at $\theta < 30°$ no regular morphology is found to develop due to a lesser degree of anisotropy in sputter erosion and also the probability of the existence of additional smoothing mechanisms operating at lower incidence angles.

ACKNOWLEDGMENT

P.M. thanks CSIR, New Delhi, for financial support.

*Corresponding author. Email address:
debabrata.ghose@saha.ac.in

[1] R. M. Bradley and J. M. E. Harper, J. Vac. Sci. Technol. A **6**, 2390 (1988).
[2] M. A. Makeev, R. Cuerno, and A. -L. Barabási, Nucl. Instrum. Methods Phys. Res. B **197**, 185 (2002).
[3] D. Flamm, F. Frost, and D. Hirsch, Appl. Surf. Sci. **179**, 95 (2001).
[4] E. Chason and M. J. Aziz, Scr. Mater. **49**, 953 (2003).
[5] P. Karmakar and D. Ghose, Nucl. Instrum. Methods Phys. Res. B **230**, 539 (2005).
[6] S. Habenicht, Phys. Rev. B **63**, 125419 (2001).
[7] U. Valbusa, C. Boragno, and F. Buatier de Mongeot, J. Phys.: Condens. Matter **14**, 8153 (2002).
[8] W. L. Chan, N. Pavenayotin, and E. Chason, Phys. Rev. B **69**, 245413 (2004).
[9] P. Karmakar and D. Ghose, Surf. Sci. **554**, L101 (2004).
[10] P. Mishra, P. Karmakar, and D. Ghose, Nucl. Instrum. Methods Phys. Res. B **243**, 16 (2006).
[11] S. Habenicht, W. Bolse, K. P. Lieb, K. Reimann, and U. Geyer, Phys. Rev. B **60**, R2200 (1999).
[12] A. Toma, F. Buatier de Mongeot, R. Buzio, G. Firpo, S. R. Bhattacharyya, C. Boragno, and U. Valbusa, Nucl. Instrum. Methods Phys. Res. B **230**, 551 (2005).
[13] P. Sigmund, J. Mater. Sci. **8**, 1545 (1973).
[14] W. W. Mullins, J. Appl. Phys. **30**, 77 (1959).
[15] P. Karmakar and D. Ghose, Nucl. Instrum. Methods Phys. Res. B **212**, 358 (2003).
[16] J. F. Ziegler, IBM Research, SRIM-2000.40 (PC version), Yorktown Heights, NY, 1999.
[17] W. Bolse, Mater. Sci. Eng. R **12**, 53 (1994).
[18] K. B. Winterbon, P. Sigmund, and J. B. Sanders, Mat. Fys. Medd. K. Dan. Vidensk. Selsk. **37**, 14 (1970).
[19] H. Oechsner, Appl. Phys. **8**, 185 (1975).
[20] F. Frost, A. Schindler, and F. Bigl, Appl. Phys. A **66**, 663 (1998).
[21] A. Hirata, H. Tokura, and M. Yoshikawa, Thin Solid Films **212**, 43 (1992).
[22] G. Carter and V. Vishnyakov, Phys. Rev. B **54**, 17647 (1996).
[23] R. Cuerno and A. -L. Barabási, Phys. Rev. Lett. **74**, 4746 (1995).
[24] B. Ziberi, F. Frost, and B. Rauschenbach, Appl. Phys. Lett. **88**, 173115 (2006).
[25] B. Ziberi, F. Frost, Th. Höche, and B. Rauschenbach, Phys. Rev. B **72**, 235310 (2005).
[26] M. Feix, A. K. Hartmann, R. Kree, J. Muñoz-Garcia, and R. Cuerno, Phys. Rev. B **71**, 125407 (2005).
[27] M. Stepanova and S. K. Dew, Appl. Phys. Lett. **84**, 1374 (2004).
[28] A. K. Hartmann, R. Kree, U. Geyer, and M. Kölbel, Phys. Rev. B **65**, 193403 (2002).